CORPUS PUBLISHERS

Journal of Mineral and Material Science (JMMS)

ISSN: 2833-3616

Volume 7 Issue 1, 2026

Article Information

Received date : February 14, 2026

Published date: March 24, 2026

*Corresponding author

Nouh SA, Department of Physics, College of Science, Taibah University, Madinah, Saudi Arabia

DOI: 10.54026/JMMS/1133

Key Words

Laser Irradiation; Poly (Allyl Diglycol Carbonate); Optical Properties; Color Changes; Dosimetry

Research Article

Enhancing Photon Detection Sensitivity in PM-355 Detectors Using a Continuous-Wave IR Laser for Dosimetric Applications

Gadallah AS[1], Ellabban MA[1], Dina G Yakot[2], Ayyash ZM[3], Al-Muubaidin HH[3], Nawaflesh OE[3] and Nouh SA[1*]

[1]*Department of Physics, College of Science, Taibah University, Madinah, Saudi Arabia*

[2]*Physics Department, Faculty of Education, Alexandria University, Alexandria, Egypt*

[3]*Students at School of Medicine, University of Jordan, Amman, Jordan*

Abstract

Poly (Allyl Diglycol Carbonate) (PADC) solid-state nuclear track detectors are widely used in radiation detection measurements. PM-355 is a commercial type pf PADC which is often optimized for better sensitivity and research applications. Our research described here is to study the feasibility of enhancing the optical properties via chain crosslinks to be used in radiotherapy quality assurance. This is due to their tissue-equivalent properties, chemical stability, and sensitivity to ionizing radiation. However, improving their photon detection sensitivity remains essential for achieving higher accuracy in clinical dose verification. In this work, laser irradiation (at exposure times ranging from 5 to 30s) is used as a treatment technique to enhance the photon detection sensitivity of PM-355 detectors. Controlled laser exposure was applied to modify the optical and structural properties of the detector material. The induced changes were systematically characterized through optical band gap analysis measurements, and colorimetric evaluation. Optical absorption spectra revealed variations in the optical band gap, indicating laser-induced modification of electronic states within the PM-355 matrix. Observable color changes provide a qualitative indicator of laser-enhanced effects. The results demonstrate that laser irradiation can effectively tailor the optical properties of PM-355 detectors, leading to improved photon sensitivity. This enhancement demonstrates potential for optimizing PM-355-based detectors in radiotherapy quality assurance applications, offering a simple and non-destructive approach for performance improvement.

Introduction

To calculate the dose of ionizing radiation, dosimeters are necessary. Therefore, ensuring that the radiation dose is accurate is essential. Any dosimeter's main goals are to guarantee cost-effectiveness, simplicity, long-term stability and ease of use [1-3]. The most popular and affordable kind of dosimeter are polymeric films, which are used in radiation processing for regular dose monitoring in dose labels and indicators. A color shift in the visible spectrum is the result of the dose being absorbed by these films [4,5]. A long-lasting color change is one of the most crucial criteria for choosing dyes and polymers in the dosimeter manufacturing process [6,7]. PM-355, often referred commercially as CR-39, remains one of the most widely used solid-state nuclear track detectors due to its high sensitivity to ionizing particles, tissue-equivalent response, and robust optical clarity [8]. In radiotherapy Quality Assurance (QA), accurate and sensitive photon detection is critical for beam characterization and dose verification, particularly as advanced treatment modalities like intensity-modulated radiotherapy and FLASH therapy demand increasingly precise dosimetric tools [9]. Although PM-355 detectors perform well for charged particle detection, their intrinsic photon sensitivity is relatively limited, which motivates research into methods for enhancing their response to photon fields [10,11].

Recent studies have shown that irradiation with external sources, including lasers and high-energy radiation, can significantly affect the optical and structural properties of polymeric detectors. A prior article, reported that controlled laser radiation on PM-355 increased optical absorbance and decreased optical band gap values, suggesting the generation of additional defect states and free radicals that can influence detector sensitivity [12]. Similarly, gamma irradiation studies on CR-39 have documented a reduction in optical band gaps with dose, indicating that ionizing radiation alters electronic structure and polarizability of the polymer matrix [13]. Laser-based modification techniques offer a promising post-processing route to tailor polymer properties without introducing chemical dopants. Laser-polymer interactions can induce chain scission, cross-linking, and defect formation, which in turn influence optical absorption edges and band structure [14]. These effects have been exploited in other polymer systems to tune optical characteristics and improve performance in optoelectronic applications, providing a conceptual foundation for their use in PM-355 detector enhancement [15].

Optical band gaps are particularly useful metrics for characterizing such modifications. Changes in the optical band gap reflect alterations in the density of electronic states and defect structures [16,17]. Moreover, observable color changes can provide a rapid qualitative indicator of polymer modifications relevant to radiation interaction and energy deposition. Integrating laser-induced modifications with quantitative optical characterization thus presents a promising approach to enhancing photon detection sensitivity in PM-355 detectors for radiotherapy QA. Several studies have been carried out on PM-355 and other solid state nuclear track detectors to enhance their optical and structural properties to be suitable candidate to dosimetry and industry [18-21]. In this study, we investigate the effects of laser irradiation on the optical properties of PM-355 detector, focusing on measurements of optical band gaps and color changes. The objective is to assess whether controlled laser treatment can enhance photon sensitivity and provide a scalable method for improving PM-355 detector performance in clinical radiotherapy environments.

Materials and Methods

Samples

Poly (allyl diglycol carbonate) sheets used in this study were manufactured by Pershore, Ltd., England. It is of density 1.32 g/cm3 and thickness 1 mm.

Irradiation tool

The laser source is a CW fiber laser operating at 1064 nm wavelength with maximum output power of 50 W. The laser diameter is 1 cm. The laser intensity during exposure was constant at 40 W/cm^2 and the exposure time varies for each sample.

Methodology

UV-Vis absorbance in the 200-800 nm wavelength range was measured utilizing an 1800 Tomos spectrophotometer that was designed by the Life Science Group, China. The CIE color alterations approach was utilized to determine the color shifts amongst the irradiated and non-irradiated samples. In our earlier paper [22] we presented all of the mathematical equations in detail.

Calculation of the tristimulus values

The CIE system is based on the description of color as luminance components X, Y and Z. Their spectral weighting curves have been standardized by the CIE based on statistics from experiments involving human observers. The magnitudes of the X, Y and Z components are proportional to physical energy, but their spectral composition corresponds to the color matching characteristics of human vision. The vision scientists created a special set of mathematical lights, X, Y and Z, to replace the actual red, green and blue lights. The color matching functions for the X, Y and Z lights are all positive numbers and are labeled $\bar{x}$, $\bar{y}$ and $\bar{z}$. Every color can be matched using the appropriate amount of X, Y and Z light. The amount of X, Y and Z light needed to match a color are called the color's tristimulus values [23].

The CIE tristimulus values for a transmitting sample are calculated by adding the product of the spectral power distribution of illuminant [24], the transmittance factor of the sample and the color matching functions of the observer at each wavelength of the visible spectrum, as shown in the following equations:

$$X = K\sum P(\lambda)\bar{x}(\lambda)T(\lambda), \quad (1)$$

$$Y = K\sum P(\lambda)\bar{y}(\lambda)T(\lambda), \quad (2)$$

$$Z = K\sum P(\lambda)\bar{z}(\lambda)T(\lambda), \text{ and } (3)$$

$$K = \frac{100}{\sum P(\lambda)\bar{y}(\lambda)} \quad (4)$$

Where P(λ) is the value of the spectral power distribution of the illuminant at the wavelength λ. T(λ) is the transmittance factor of the sample at the wavelength λ and $\bar{x}$ (λ), $\bar{y}$ (λ) and $\bar{z}$ (λ) are the CIE color matching functions for the standard observer at the wavelength λ. The factor k normalizes the tristimulus value so that Y will have a value of 100 for a perfect white diffuser.

Calculation of the chromaticity coordinates

It is often convenient to discuss pure color in the absence of brightness.
The CIE defines a normalization process to compute little x, y and z chromaticity coordinates that specify the saturation according to the following equations:

$$x = \frac{X}{X+Y+Z}, \quad (5)$$

$$y = \frac{Y}{X+Y+Z}, \text{ and } (6)$$

$$z = \frac{Z}{X+Y+Z}, \quad (7)$$

Calculation of the color difference

A weakness of the CIE X, Y and Z color system is its lack of visual uniformity. Creating a uniform color space would have two major advantages. It would allow plots showing the perceptually relative positions of two or more colors in color space, and it would facilitate the creation of a good color difference ruler between two samples. The 1976 CIE L* a* b* color space is widely used in the paint, plastic and textile industries. The L*, a*, b* intercepts used in this system are based on the CIE color triangle. In this system, the L* value specifies the dark-white axis, a* the green-red axis, and b* the blue-yellow axis. The CIE L*, a* and b* coordinates are calculated from the tristimulus values according to the following equations:

$$L* = 116f\left(\frac{Y}{Yn}\right) - 16, \quad (8)$$

$$a* = 500\left[f\left(\frac{X}{Xn}\right) - f\left(\frac{Y}{Yn}\right)\right], \text{ and } (9)$$

$$b* = 200\left[f\left(\frac{Y}{Yn}\right) - f\left(\frac{Z}{Zn}\right)\right], \quad (10)$$

In which X, Y and Z are the tristimulus values and the subscript n refers to the tristimulus values of the perfect diffuser for the given illuminant and standard observer; $f\left(\frac{X}{Xn}\right) = \left(\frac{X}{Xn}\right)^{1/3}$ for values of $\left(\frac{X}{Xn}\right)$ greater than 0.008856 and $f\left(\frac{X}{Xn}\right) = 7.787\left(\frac{X}{Xn}\right) + \frac{16}{116}$ for values of $\left(\frac{X}{Xn}\right)$ equal to or less than 0.008856; and the same with Y and Z replacing X in turn.

The CIELAB color difference, ΔE is given by:

$$\Delta E = [(L_1^* - L_2^*)^2 + (a_1^* - a_2^*)^2 + (b_1^* - b_2^*)^2]^{\frac{1}{2}} \quad (11)$$

Results and Discussion

Optical investigation

Absorption study: The UV absorbance spectra of the pristine and irradiated PM-355 films are shown in Figure 1 to study the alterations in the bandgap (E_g) configuration due to the laser irradiation and to obtain information about the optical microelectronic transitions. The reduction of absorption with increasing wavelength can be attributed to decreasing number of possible (n– π*) carbonyl group and phenyl group (π– π*) transitions [17].

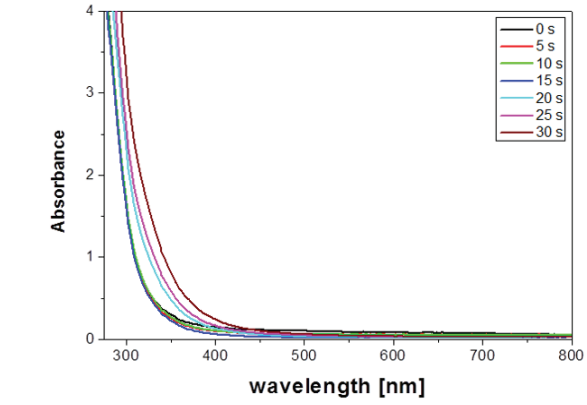

Figure 1: The UV–Vis absorbance spectra of the pristine and irradiated PM-355 films.

Moreover, the absorbance rise of the PM-355 films on increasing the laser exposure time up to 30s can be assigned to the development of bonding as a result of chain crosslinks [25-28].

Bandgap investigation: For dosimetric purposes, an appropriate property to be used is the decrease of the energy of the optical band gap as a function of the γ ray dose. The optical band gap is suitable to be used as a parameter in γ ray dosimetry. These kind of passive dosimetry methods are suitable for many applications involving high gamma-rays doses [29-32]. Accordingly, we measured the optical band gap and studied its dependence on the γ ray dose.

The bandgap (Eg) values were calculated applying Tauc's principle [33]:

$$\alpha h\nu = B(h\nu - E_g)^n \quad (12)$$

where hν is the photon energy, B is a constant and the index n has a value that signifies the character of the microelectronic transition. In the case of a direct transition, n is valued at 1/2 or 3/2, while in the case of an indirect transition n is valued at 2 or 3, according to whether being allowed or forbidden for each pair of values [34]. The values of E_g were determined by plotting $(\alpha h\nu)^{\frac{1}{n}}$ versus $h\nu h\nu$ and then extending the straight portion of the plot at $h\nu h\nu$ axis (Figure 2 & 3).

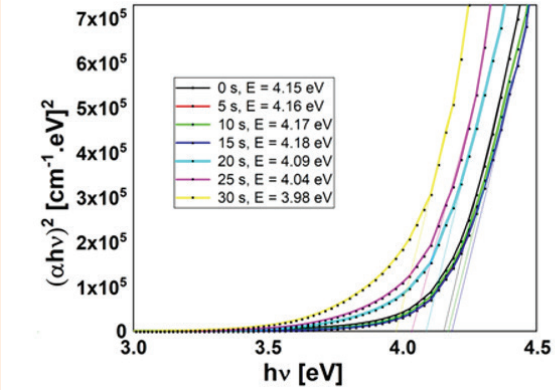

Figure 2: A plot of $(\alpha h\nu)^2$ versus hν for the pristine and irradiated PM-355 films.

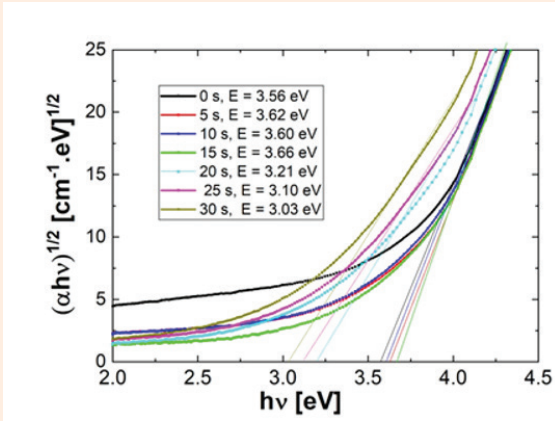

Figure 3: A plot of $(\alpha h\nu)^{1/2}$ versus hν for the pristine and irradiated PM-355 films.

The variation of direct E_g of the PM-355 films with the laser exposure time is shown in Figure 4. The E_g values increasing upon increasing the laser exposure time 15s and then decreased with increasing the exposure time up to 30s. The interpretation of these results can be as follows: when the polymeric detector suffers laser exposure up to 15s, its degree of ordering or its crystallization will be enhanced due to chain scissions. In other words, the exposure of the polymeric detector to laser raises the surface to the vaporization temperature and begins to vaporize. The evaporated material will flow away because of the thermal gradient leaving behind it a resultant pit. After stopping the stimuli, the molten material begins to recrystallize at the colder regions in the surrounding of the pit. This leads to the growth of crystalline regions due to degradation, meaning the breaking of chemical bonds in the polymer chains. Consequently, free radicals are formed, which then recombine to create crosslinks between chains. This crosslinking improves the stability of the polymeric detector and its sensitivity to photons registration [35].

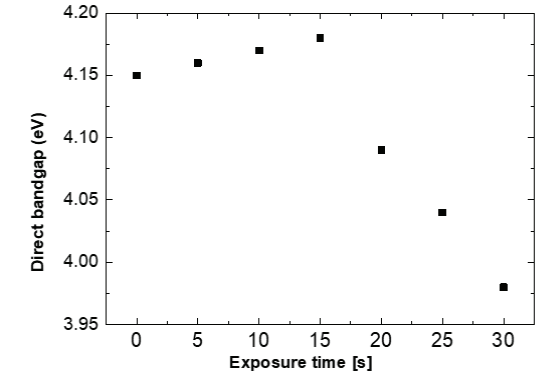

Figure 4: Variation of E_g with the laser exposure time.

Color difference measurements

An important characteristic of the color appearance of nuclear track detectors is the evaluation of color difference with variation in the laser exposure time. The color parameters were calculated using the transmission records (370-780 nm), computed from the absorbance spectra (Figure 5).

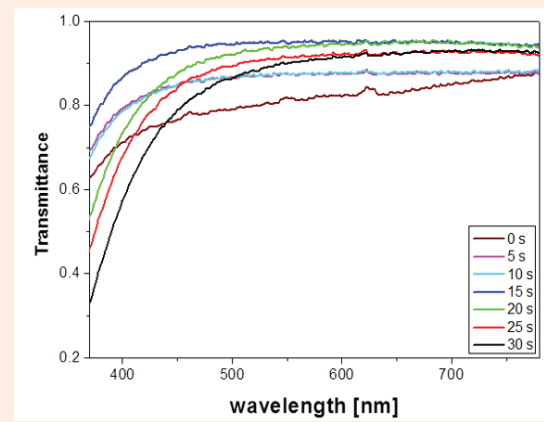

Figure 5: The transmission spectra of the pristine and irradiated PM-355 films.

The chromaticity coordinates and tristimulus values were estimated and are given in Table 1 at different laser exposure time. The X, Y and Z values decrease with increasing exposure time up to the maximum 30s. The coordinates x and y increase on increasing the exposure time up to 30s, whereas the z coordinate exhibits a reverse trend.

Table 1: The tristimulus values (X, Y and Z) and chromaticity coordinates (x, y and z) of the PM-355 films at different laser exposure times.

Exposure Time (s)	Tristimulus Values			Chromaticity Coordinates		
	X	Y	Z	x	y	z
0	87.04	89.75	95.89	0.3012	0.3345	0.3605
5	86.94	89.32	95.61	0.3038	0.3362	0.3592
10	86.73	89.01	95.13	0.3063	0.3371	0.3568
15	86.88	88.84	94.45	0.3092	0.3322	0.3662
20	86.54	88.43	94.31	0.3105	0.3393	0.3532
25	86.23	88.26	94.52	0.3128	0.3403	0.3548
30	86.12	88.17	94.03	0.31.72	0.3445	0.3512

The intercept a* denotes the green–red axis, whereas the intercept b* denotes the blue–yellow axis. L* specifies the dark–white axis. L* is valued 100 for the perfect white, and is valued 0 for the perfect black. The accuracy in estimating L˙ is ±0.05 and is ±0.01 for both a* and b*, respectively. The variations of a*, b* and L* with the laser exposure time are presented in Table 2.

The intercepts b* increased with increasing the exposure time up to 30s, signifying the tendency of the blue color constituents to become yellow. The intercept a* exhibited similar values within experimental error, meaning that the green-red components didn't affected by the laser irradiation. This was related to the growth in darkness in the samples as indicated from the decrease of L*.

Table 2: The color intercepts (L*, a* and b*) and the color intensity (ΔE) of the PM-355 films at different laser exposure times.

Exposure Time (s)	Color Intercepts			Color Intensity
	L*	a*	b*	ΔE
0	97.22	0.40	0.36	0
5	97.04	0.41	0.52	0.241039
10	96.83	0.39	0.61	0.463357
15	95.42	0.38	0.83	1.860457
20	95.23	0.42	0.85	2.049537
25	94.16	0.41	0.94	3.114498
30	93.10	0.38	0.97	4.164961

The color intensity (ΔE), representing the color difference between the irradiated films and pristine, was estimated using the 1964 CIE color difference equation [22] and is given in Table 2 as a function of exposure time. The values of ΔE increased with increasing the exposure time up to 30s. The color intensity reached a value of 4.1. This is an acceptable match in commercial reproduction on printing presses [36,37]. The change in color can be attributed to the hot free radicals that are formed by ionization, so the change in color is associated with many morphological changes in the polymer, such as (i) the disorder of the dissocyanate groups (which form the hard segments of the polymer) and (ii) the damage to chain extenders which join the different groups of the hard segments. The main factors responsible for coloration are the formation of conjugated double bonds and free radicals. The former produces the unsaturation which has electron excitation levels in the visible spectral range and will also produce discoloration and reduction in light transmission. Furthermore, the trapped free radicals produced from radiation induced rupture of polymer molecules, have electrons with unpaired spins. Such species may also give optical coloration [22].

Conclusion

The laser exposure of PM-355 films in the exposure time range 15-30s caused crosslinking that enhanced their optical absorbance, the optical bandgaps and hence enhanced its photon's registration sensitivity. This was accompanied by modifications in the color that optimized the PM-355 to be a suitable candidate for dosimetric applications in several medical applications.

References

1. Soliman YS, Beshir W, Abdel-Fattah A, Fahim RA, El-Anadouli BE (2016) Radiation-induced coloration of xylenol blue/film containing hexachloroethane for food irradiation applications. J Radioanal Nucl Chem 310: 117-124.
2. Doyan A, Susilawati S, Prayogi S, Bilad MR, Arif MF, et al. (2021) Polymer film blend of polyvinyl alcohol, trichloroethylene and cresol red for gamma radiation dosimetry. Polymers 13: 1866.
3. Moftah B, Basfar AA, Almousa AA, Al Kafi AM, Rabaeh KA (2020) Novel 3D polymer gel dosimeters based on N-(3-Methoxypropyl) acrylamide (NMPAGAT) for quality assurance in radiation oncology. Radiat Meas 135: 106372.
4. Soliman YS, Beshir WB, Abdelgawad MH, Bräuer-Krisch E, Abdel-Fattah AA (2019) Pergascript orange-based polymeric solution as a dosimeter for radiotherapy dosimetric validation. Phys Med 57: 169-176.
5. Harahap M, Widodo P, Priasetyono Y, Listyarini A, Djuhana D, et al. (2019) Simple gamma dosimeter using a film label made of polyvinyl alcohol and bark of peltophorum ferrugineum extract. IOP Conf Ser Mater Sci Eng 496: 012041.
6. Abdel-Fattah AA, Soliman YY, Bayomi AM, Abdel-Khalek AA (2014) Dosimetric characteristics of a radiochromic polyvinyl butyral film containing 2,4-hexadiyn-1,6-bis (n-butyl urethane). Appl Radiat Isot 86: 21-27.
7. El-Malawy Al-Abyad DM, Ghazaly MEl, Abdel Samad S, Hassan HE (2021) γ-ray effects on PMMA polymeric sheets doped with CdO nano particles. Radiat Phys Chem 184: 109463.
8. Alkhayat RB, Zakar AT, Al-Jubbori MA, Hasan HI (2025) Laser radiation detection of the fluctuation alpha particle tracks in PADC. Results in Physics 75: 108342.
9. Shaikh S, Escribano-Rodriguez S, Radogna R, Saakyan R, Manger S, et al. (2025) Range quality assurance measurements for clinical and FLASH proton beam therapy using the quality assurance range calorimeter. Frontiers on Oncology 15: 1622231.
10. Sapkal J (2024) Assessment of etching and optical characteristic of an indigenously prepared poly allyl diglycol carbonate solid-state nuclear track detector material on gamma irradiation and its applicability in gamma dose measurements. Radiation Protection and Environment 47: 224-228.
11. Sadeq MS, Hassan NM, El-Saftawy AA, Sedqy EM (2024) Studies of chemical bonds loss and optical modifications of CR-39 caused by gamma rays. Radiation Physics and Chemistry 218: 111537.
12. Al-Jubbori MA, Alkhayat RB, Ali MH, Mahmood RW (2025) UVC irradiation of alpha particles tracks and empirical equation of bulk etch rate in CR-39 detector. Nuclear Instruments and Methods in Physics Research B 559: 165596.
13. Othman SM, El-Mesady IA, El-badawy AS, Ghanim EH (2024) The impact of the broad range of gamma doses on follow-up fission fragment track parameters in CR-39 radiation detector, Applied Radiation and Isotopes 208: 111253.
14. Saad AF, Sedqy EM, Ahmed RM (2021) Effect of UVC radiation on the optical properties of thermally treated CR-39 polymer films: A new approach for the use of CR-39 as an optical dosimeter. Radiation Physics and Chemistry 179: 109253.
15. Mamand DM, Aziz DM, Khasraw SS, Al-Azzawi AGS, Al-Saeedi SI, et al. (2025) Improved optical characteristics of PEO polymer integrated with graphene oxide. Scientific Reports 15: 32225.
16. Traynor NBJ, McLauchlin C, Dodge K, McGarrah JE, Padalino SJ, et al. (2018) CR-39 (PM-355) reflection and transmission of light in the ultraviolet-near-infrared (UV-NIR) range. Applied Spectroscopy 72(4): 591-597.
17. Bashir S, Ahmad S, Ali N, Kalsoom U, Rafique MS, et al. (2024) Modification in electrical conductivity correlated with surface, structural & optical characteristics of graphite ions implanted CR-39. Heliyon 10: e34553 (2024).
18. Nouh SA, Alghamdi EE, Gaballah NS, Eldera SS, AlSomali F, et al. (2025) Tailoring the optical and color properties of gamma-irradiated PC/CuO nanocomposite films for their application in optoelectronic devices. Radiation Effects and Defects in Solids 180: 209-226.
19. Nouh SA, Gweily N, Al Somal F, Bahareth RA, Barakat MM 2025) Tailoring the optical and color properties of gamma irradiated polycarbonate/cerium oxide nanocomposite films for their application in optoelectronic devices. Journal of Macromolecular Science Part B 64: 1667-1682.

20. Nouh SA, Alsufyani SJ, Gweily N, Chaitali VM, Barakat MME (2025) Gamma ray irradiation induced changes in polycarbonate/ zinc sulfide-cerium oxide nanocomposite films. Optical and color modifications. Journal of Macromolecular Science Part B 1-16.

21. Nouh SA, Mahrous EM, AlSomali F, Yajzey R, Benthami K, et al. (2023) Optical and color modification in polycarbonate/zns-nio nanocomposite films due to laser exposure. J Russ Laser Res 44: 597-608.

22. Tommalieh MJ, Barakat MM, Bahareth RA, Mahrous EM, Saad D, et al. (2022) Optical, and color modification in makrofol VLG 7-1 nuclear track detector due to gamma irradiation. Journal of Macromolecular Science Part B: Physics 61(3): 479-493.

23. Nassau K (1998) Color for Science, Art and Technology. Elsevier, New York, USA.

24. El-Mesady IA, Rammah YS, Abdalla AM, Ghanim EM (2020) Gamma irradiation effect towards photoluminescence and optical properties of makrofol DE 6-2. Radiat Phys Chem 168: 108578.

25. Nouh SA, Benthami K, Abou Elfadl A, El Shamy NT, Tommalieh MJ (2021) Structural, thermal and optical characteristics of laser-exposed Pd/PVA nanocomposite. Polym Bull 78: 1851-1866.

26. Alosaimi AM, Barakat MM, Ellabban MA, Abbady G, Gadallah AS, et al. (2025) Impact of gamma ray irradiation on the structural, linear and nonlinear optical properties of polycarbonate/polyethylene oxide/poly (methyl methacrylate)/ chromium oxide nanocomposite membranes for their application in optoelectronics. J Radiat Res Appl Sci 18: 102091.

27. Nouh SA, Ellabban MA, Algethami M, Alsomali FA, Barakat MM (2025) Color changes and optical properties of gamma irradiated polycarbonate/poly (methyl methacrylate)/polyvinyl chloride blended polymers: Linear and nonlinear optical parameters. J Radiat Res Appl Sci 18(4): 101893.

28. Nouh SA, Aldawood S, Barakat MM, Tommalieh MJ, Bahareth RA (2022) Laser-induced changes in the optical properties of the bayfol UV1 7-2 nuclear track detector. Radiat Eff Defects Solids 177: 57-70.

29. Tugulan LC, Ioan GV (2020) Optical band gap as parameter in gamma-rays dosimetery (high doses). Rom Rep Phys 72: 803.

30. Negoita F, Roth M, Thirolf PG, Tudisco S, Hannachi F, et al. (2016) Laser driven nuclear physics at ELI-NP. Rom Rep Phys 68: S37-S144.

31. Homma K, Tesileanu O, D'alessi L, Hasebe T, Ilderton A, et al. (2016) Combined laser gamma experiments at ELI-NP. Rom Rep Phys 68: S233-S274.

32. Asavei T, Tomut M, Bobeica M, Aogaki S, Cernaianu MO, et al. (2016) Materials in extreme environments for energy, accelerators and space applications at ELI-NP. Rom Rep Phys 68: S275-S347.

33. Tauc J (1972) Optical Properties of Solids. In: Abeles F (Ed.), Amsterdam: North-Holland, Netherlands. p. 77.

34. Aziz SB, Abdullah OG, Hussein AM, Ahmed HM (2017) From insulating PMMA polymer to conjugated double bond behavior: Green Chemistry as a novel approach to fabricate small band gap polymers. Polymers 9(11): 626.

35. Alharby TS, Barakat MM, Nouh SA, Yakot DG (2025) Laser induced alterations in the optical and color properties of polycarbonate/ poly (methyl methacrylate)/ polybutylene terephthalate polymer composite. Journal of Macromolecular Science Part B 1-17.

36. Benthami K, Barakat MM, Nouh SA (2020) Modification of optical properties of PC-PBT/Cr_2O_3 and PC-PBT/CdS nanocomposites by gamma irradiation. Eur Phys J Appl Phys 92: 20402.

37. Nouh SA, Barakat MM, El-Nabrawy HA, Benthami K, Elhalawany N (2021) Color changes in some uv irradiated polymer nanocomposite materials for the application in textile industry. Fibers Polym 22: 1711-1717.